Citation for published version:
Chuck, CJ, Bannister, CD, Jenkins, RW, Lowe, JP & Davidson, MG 2012, 'A comparison of analytical techniques and the products formed during the decomposition of biodiesel under accelerated conditions', *Fuel*, vol. 96, pp. 426-433. https://doi.org/10.1016/j.fuel.2012.01.043

DOI:
10.1016/j.fuel.2012.01.043

Publication date:
2012

Link to publication

NOTICE: this is the author's version of a work that was accepted for publication in Fuel. Changes resulting from the publishing process, such as peer review, editing, corrections, structural formatting, and other quality control mechanisms may not be reflected in this document. Changes may have been made to this work since it was submitted for publication. A definitive version was subsequently published in Fuel, 96, 1, 2012
DOI:10.1016/j.fuel.2012.01.043

University of Bath

Alternative formats
If you require this document in an alternative format, please contact:
openaccess@bath.ac.uk

General rights
Copyright and moral rights for the publications made accessible in the public portal are retained by the authors and/or other copyright owners and it is a condition of accessing publications that users recognise and abide by the legal requirements associated with these rights.

Take down policy
If you believe that this document breaches copyright please contact us providing details, and we will remove access to the work immediately and investigate your claim.

Download date: 05. May. 2023

A comparison of analytical techniques and the products formed during the decomposition of biodiesel under accelerated conditions

Christopher J. Chuck,[a]* Chris D. Bannister,[b] Rhodri W. Jenkins,[a] John P. Lowe[c] and Matthew G. Davidson[a,c]

[a] Centre for Sustainable Chemical Technology, Department of Chemistry, University of Bath, Bath, UK, BA2 7AY.

[b] Department of Mechanical Engineering, University of Bath, Bath, UK, BA2 7AY.

[c] Department of Chemistry, University of Bath, Bath, UK, BA2 7AY.

*email C.Chuck@bath.ac.uk, tel: +44 (0)1225 383537, fax: +44 (0)1225 386231

Introduction

Biodiesel, the alkyl esters derived from the transesterification of plant, animal, waste or algal lipids, can be used as a direct substitute for diesel fuel. However, a number of issues such as the reduced oxidative stability restrict the applications and acceptable blend level of biodiesel. Unlike diesel fuel, biodiesel is prone to oxidation leading to an increased viscosity and cetane number, a reduced heating value and eventually the production of insoluble particles and gums in the fuel [1].

Biodiesel derived from rapeseed, soybean or palm oil is made up of six main fatty acid alkyl esters: palmitic acid, C16:0, palmitoleic acid, C16:1, stearic acid, C18:0, oleic acid, C18:1, linoleic acid, C18:2, and linolenic acid, C18:3. Biodiesel derived from microalgae also contains a variety of other FAME types with generally longer chain lengths and higher levels

of unsaturation [2]. Fuels with higher proportions of polyunsaturated components are more unstable to oxidation than those containing monounsaturated components which in turn are more prone to degradation than those with saturated components. The rate of degradation are also affected by light and temperature. This is reflected in the Rancimat testing of these fuels, where soybean oil methyl ester gives a lower value than rapeseed methyl ester which in turn is less stable than palm oil methyl ester [3].

The oxidation of biodiesel is a major issue as the oxidised fuel can block filters and injectors which in turn leads to fuel starvation and poor combustion. Oxidised fuel can also have a detrimental effect on the engine architecture and operation including producing an acidic, corrosive environment within the fuel delivery system that can result in fuel injection equipment failure [4]. Biodiesel also has a tendency to accumalate in the engine sump oil, especially in vehicles fitted with a diesel particulate filter (DPF) system. Unlike mineral diesel, which will evaporate from the lubricating oil under normal operating temperatures, biodiesel sourced from terrestrial crops high in long chain fatty acid esters will not and instead oxidises leading to a significant increase in the viscosity necessitating a premature oil change [5-7].

A number of mechanisms have been proposed detailing how biodiesel can degrade [1]. The primary mechanism, the auto-oxidation, proceeds with the formation of a radical hydrocarbon species on the bisallylic carbon. The double bonds will isomerize into a conjugated structure. This radical can then react with oxygen to form a peroxide species propagating the reaction. The peroxides are thought to break down into oxygenated intermediates which further degrade into small chain acids, ketones, alkenes and aldehydes [8]. The peroxide species' can also form dimers and oligomers via peroxy, ether or carbon-carbon bonds [9]. Recently, further evidence has suggested that the propagating species is

not a monosubstituted hydroperoxide but an oligomeric species with more than one peroxide linker which propagates the reaction by rapidly breaking down into aldehydes, acids and a radical alcohol [10]. This is not the only reaction path discussed however, and it is thought that a saturated and unsaturated aldehyde can be formed on the decomposition of a biodiesel chain with more than one peroxide group [11].

In order to aid development of methods to improve the oxidative stability of biodiesel fuel knowledge about the mechanism by which it degrades is important. In the first case it will aid in the development of simple sensors to assess the oxidative stability. Secondly it will allow a targeted approach to synthesising antioxidants and, finally, a better understanding will be gained into the validity of accelerated testing. To this end, in this research paper, RME was oxidised over 360 hours at both 90 and 150 °C. Though these temperatures are higher than observed on biodiesel storage they are normal operating conditions for the lubricant oil in the engine sump. To measure the course of the reaction aliquots were taken and were analysed by GC-MS, ^{1}H and ^{13}C NMR spectroscopy including COSY, TOCSY and HMQC experiments, UV-VIS spectroscopy, FT-IR spectroscopy, the dynamic viscosity, GPC and the refractive index. The data obtained were compared and correlated to better understand the mechanisms of decomposition occurring, to determine the exact nature of the major oxidative products and to determine the most promising technique to produce a simple oxidative sensor.

2 Experimental

2.1 Materials

Rapeseed methyl ester was supplied by BP. Deuterated solvents were obtained from flurochem. Chloroform, hexane and methanol were purchased from Sigma Aldrich. All chemicals were used without any further purification.

2.2 Methods

2.2.1 Test procedure

A three necked flask was charged with RME (400 ml, 349.6 g) and biphenyl (1.8 g, 0.0117 mols) was added as an internal standard. The flask was placed in a graphite heating bath set to the required temperature and the solution was mechanically stirred at a constant rate. Air was bubbled through the reaction mixture at a rate of 1000 ml min^{-1} via a stainless steel needle inserted through a seal. Volatile components were collected via a reflux condenser into a small trap filled with deuterated water. 5 ml aliquots were taken at 0, 8, 24, 32, 48, 56, 72, 80, 96, 104, 120, 128, 144, 152, 168, 176, 192, 200, 216, 224, 240, 248, 264, 272, 288, 296, 312, 320, 336, 344 and 360 hours from the main reaction, culminating in the removal of 150 ml from the original 400 ml. The deuterated water was replaced. The collected D_2O aliquot was analysed by NMR spectroscopy after methanol (0.01 g) was added as a calibrant. All aliquots were stored at -85 °C prior to analysis to prevent any further oxidation.

2.2.2 NMR spectroscopy

NMR spectroscopic measurements were carried out at 298 K using a Bruker AV500 spectrometer, operating at 500.13 MHz for ^{1}H and 125.76 MHz For ^{13}C. Typically samples were made up of 0.05 ml of oxidised biodiesel dissolved in 0.5 ml $CDCl_3$, or alternatively 0.5

ml of the D_2O trap with an additional 0.1 g of methanol added as an internal calibrant. ^1H spectra were typically acquired using a 30 degree excitation pulse and a repetition time of 4.2 sec. 0.3 Hz line broadening was applied before Fourier transform, and spectra were referenced to the residual $CHCl_3$ peak from the solvent (δ 7.26 ppm). COSY, HMQC and 1D (zero-quantum suppressed) TOCSY experiments were acquired using standard Bruker pulse sequences ; the latter used an MLEV-17 spin-lock applied for 100 ms.

2.2.3 FT-IR Spectroscopy

FT-IR measurements were undertaken using a Bruker Matrix MF spectrometer equipped with HeNe MIR probe IN350-T, at room temperature. Integration program C was used in the OPUS 6.1 software process package for analysis.

2.2.4 UV-VIS Spectroscopy

Samples were dissolved in chloroform (1:50 by volume) and the UV measurements were collected on a Perkin Elmer Lambda UV–Vis Spectrometer. All data was collected in the 200-750 nm range.

2.2.5 Dynamic Viscosity

The dynamic viscosity over the kinematic viscosity was selected to analyse the samples due to the extremely high viscosities reached over the course of the experiment. The viscosity of the samples were measured using a Bohlin GeminiRotonetic Drive2 rotating disk rheometer. All viscosity measurements were obtained using the in-built temperature controller in the range 15 to 40 °C.

2.2.6 Refractive Index

The refractive index was measured using a Bellingham and Stanley 586269 refractometer, referenced to water (20 °C, *n* = 1.333) and methyl oleate (20 °C *n* = 1.452).

2.2.7 Gas Chromatography-Mass Spectroscopy

GC-MS analysis was carried out using an Agilent 7890A Gas Chromatograph equipped with a capillary column (60m × 0.250mm internal diameter) coated with DB-23 ([50%-cyanpropyl]-methylpolysiloxane) stationary phase (0.25µm film thickness) and a He mobile phase (flow rate: 1.2ml/min) coupled with an Agilent 5975C inert MSD with Triple Axis Detector. A portion of the biodiesel samples (approximately 50mg) was initially dissolved in 10ml dioxane and 1µl of this solution was loaded onto the column, pre-heated to 150°C. This temperature was held for 5 minutes and then heated to 250°C at a rate of 4°C/min and then held for 2 minutes. The peak area was normalised using the biphenyl internal standard peak area.

2.2.8 Gel Permeation Chromatography

Gel Permeation Chromatography (GPC) analyses were performed on a Polymer Laboratories PL-GPC 50 integrated system using a PLgel 5 µm MIXED-D 300 x 7.5 mm column at 35 °C, THF solvent (flow rate, 0.8 ml/min).

3 Results and Discussion

The rapeseed methyl ester used throughout this study fell within the specifications of EN14 214, has a standard FAME profile for RME and a Rancimat induction time of 11 hours (Tables 1 & 2).

3.1 NMR spectroscopy

3.1.1 Oxidised biodiesel

Several previous studies have detailed the applicability of ^{1}H NMR spectroscopy in assessing the decomposition of biodiesel [12,13]. The terminal CH_3 protons of the 18:3 fatty acid (δ 0.9 ppm) can be quantified, as can the bisallylic protons (δ 2.3 ppm), the CH_3 group of the methyl ester (δ 3.6 ppm) and the double bonds (δ 5.4 ppm) can also be assessed (fig. 1). Using these shifts, the decomposition of the unsaturated components could be assessed (fig. 2a).

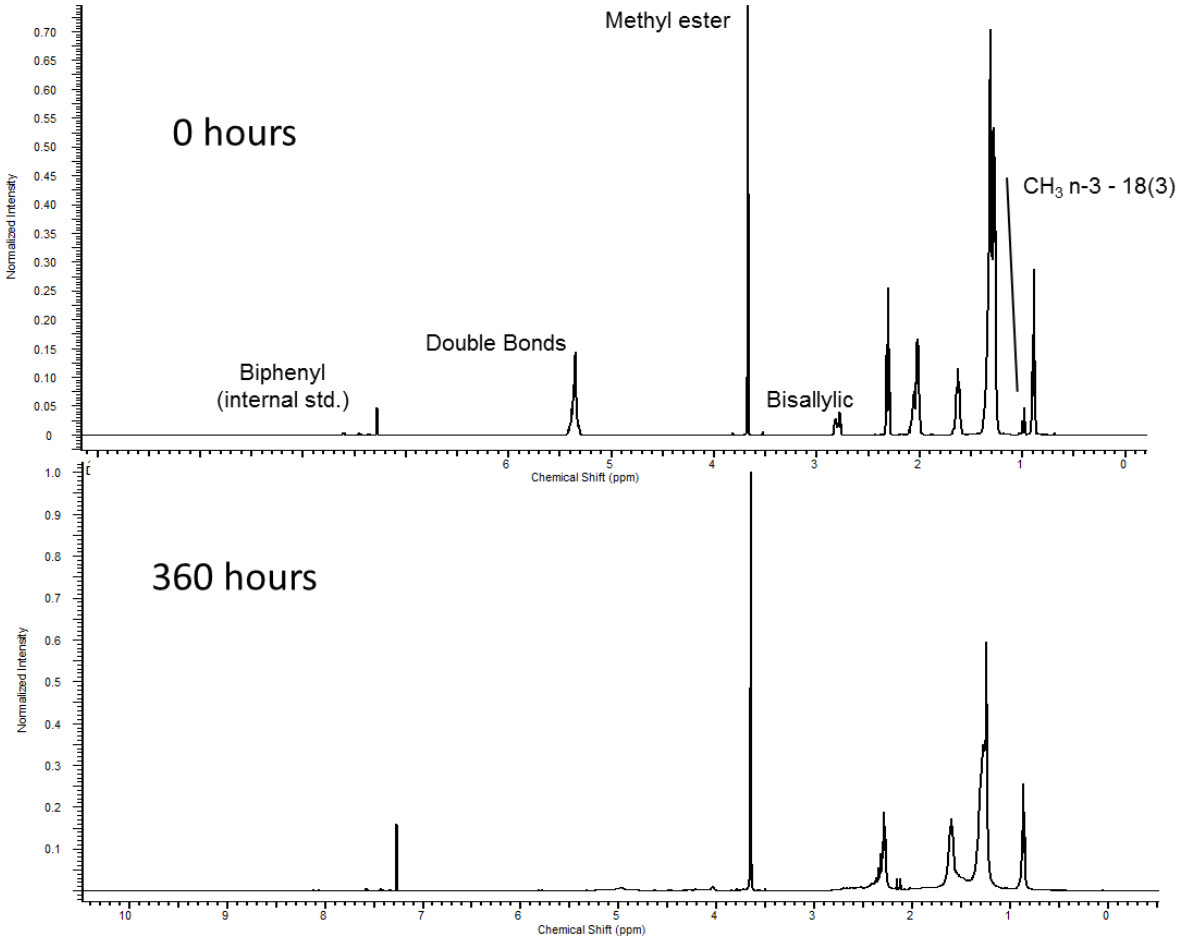

Fig. 1 ^{1}H NMR spectra of the degradation of RME at 150 °C taken at 0 and 360 hours.

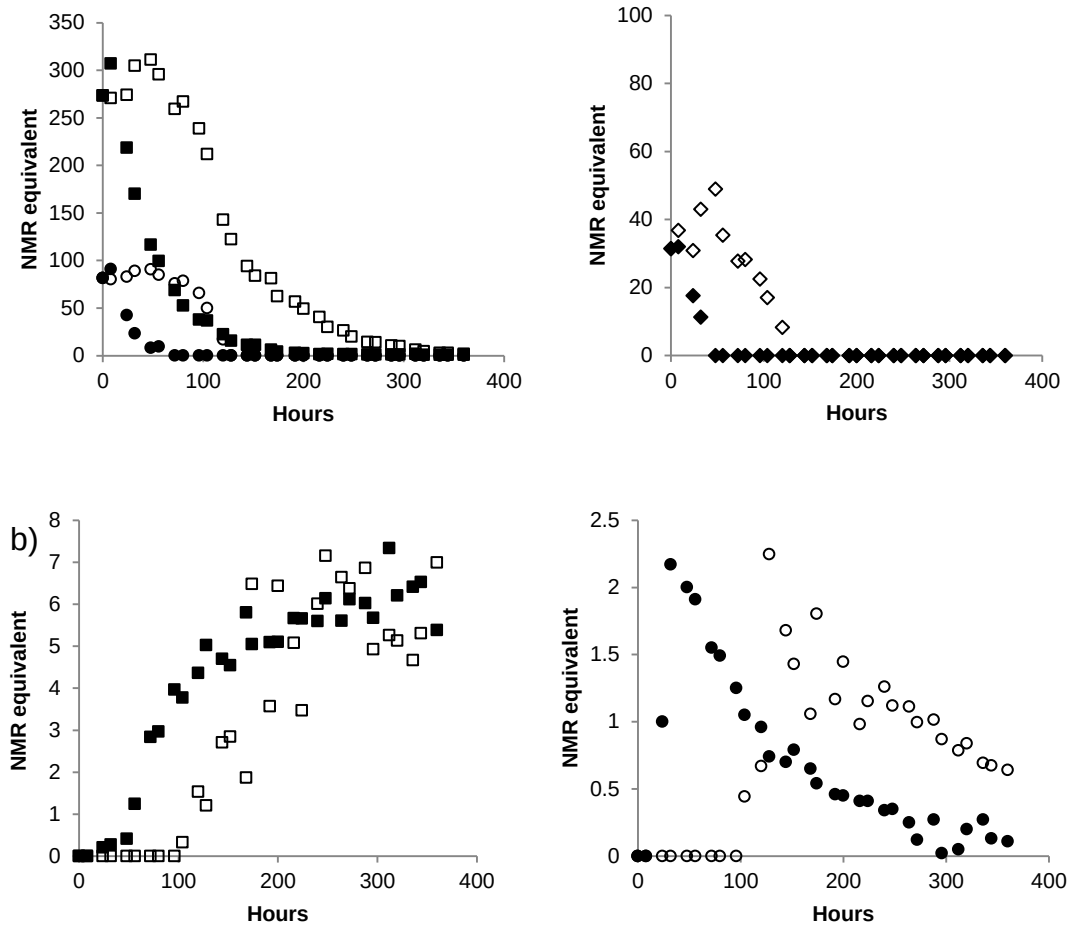

Fig. 2 a) Reduction in the double bonds (□), bisallylic protons (○) and linolenic acid terminal CH_3 group (◊) in the oxidation of biodiesel. b) Formation of formic acid and formates (□) and aldehydes (○) throughout the reaction. Solid blocks show the degradation at 150 °C, clear blocks at 90 °C.

The peak assignable to the CH_3 group of the ester remained constant throughout the reaction. Therefore, the ester moiety is not reacting with atmospheric moisture or alcohols, formed during the course of the reaction, to any significant degree, and rather a series of oxygenated esters are being formed on decomposition. From the change in the peaks relating to the unsaturates, it is clear that the oxidation of biodiesel at 150 °C is already underway within 24 hours, this induction period lengthens to 80 hours when the temperature is reduced to 90 °C. Within 48 hours, at 150 °C, less than 1% of the 18:3

remains, within 72 hours there is no longer a signal corresponding to the bisallylic peak suggesting there is no 18:2 remaining, and within 192 hours there are no unsaturated fatty acids remaining in the reaction mixture. This process is also observed, albeit less quickly, in the 90 °C test. After 80 hours the antioxidant has been consumed and the oxidation begins. Within an additional 72 hours there are no polyunsaturates present in the mixture and by the 320 hour mark there are no unsaturated esters remaining at all.

It is also possible to analyse some of the oxygenated decomposition products by ^{1}H NMR. The resonances from the protons of conjugated bonds appear at δ 6.0-6.4 ppm, aldehydes have characteristic shifts at δ 9.4-10.0 ppm, while formic acid and formate species will give a characteristic resonance at around δ 8 ppm (fig. 2b). While other studies have suggested that the peroxide species can also be observed [14], the peaks visible in the spectra between δ 3.8 - 4.5 ppm could not be assigned with any confidence and are probably a large mixture of different components including alcohols.

As expected conjugated bonds are observed at the start of the reaction though quickly disappear within the first few samples. Aldehydes, one of the degradation products of peroxide decomposition are observed after 24 hours in the 150 °C reaction. They reach a maximum at 48 hours and steadily decline throughout the rest of the reaction time. A similar trend is observed in the 90 °C reaction with aldehydes being observed after 96 hours, reaching a maximum at 128 hours before declining steadily. Similar quantities of aldehydes are observed in both reactions. The maximum level of aldehydes in both reactions corresponds with the decomposition of the bisallylic sites. This suggests that aldehydes are primarily formed by the degradation of peroxides produced by the breakdown of the polyunsaturated FAME and then degrade into further oxygenates as the reaction continues.

Several aldehydes are seen in the ^{1}H spectrum, at around δ 9.7 and 9.5 ppm The major species observed early on in the reaction is seen as a doublet (J = 7.9 Hz) at 9.50 ppm. This doublet relates to an unsaturated aldehyde, confirmed by the corresponding COSY and TOCSY plots which show the protons are coupled to unsaturated protons at δ 6.11 and δ 6.84 ppm. The coupling constant between the alkenic protons, 15.1 Hz, is characteristic of a double bond in a *trans* formation (see supporting information). Unsaturated aldehydes have a distinctive pungent aroma and it is likely that this compound adds to the characteristic smell of oxidised biodiesel.

Formic acid is produced on the decomposition of biodiesel and, although it is distilled from the reaction mixture, it can also react with alcohols, a likely by-product of the oxidation, resulting in formates. The production of multiple formates is confirmed by the corresponding COSY plot (see supporting information) and is observed in both reactions. The production of formates corresponds to the start of degradation of the polyunsaturated FAME but continues after this feedstock has been exhausted. There will be numerous reactions producing alcohols, as well as formic acid, beyond this point as the secondary oxygenated products break down further. As there are many different formates, all of which will have unique formation and degradation rates, there is no clear trend in their overall production.

3.1.2 Volatiles

The volatiles given off throughout the reaction were collected in a D_2O trap and analysed by ^{1}H NMR. When biodiesel degrades volatile organic acids are produced, the measurement of these acids forms the basis of the Rancimat test [15]. In a previous study, the elution of formic acid and acetic acid were observed on holding various FAME samples at 120 °C over

20 hours [16]. However, in the course of the reactions undertaken at both 90 and 150 °C formic acid, acetic acid and propionic acid were all observed and quantified (fig. 3). A number of larger, branched organic acids were also observed - though in amounts too small to be quantifiable.

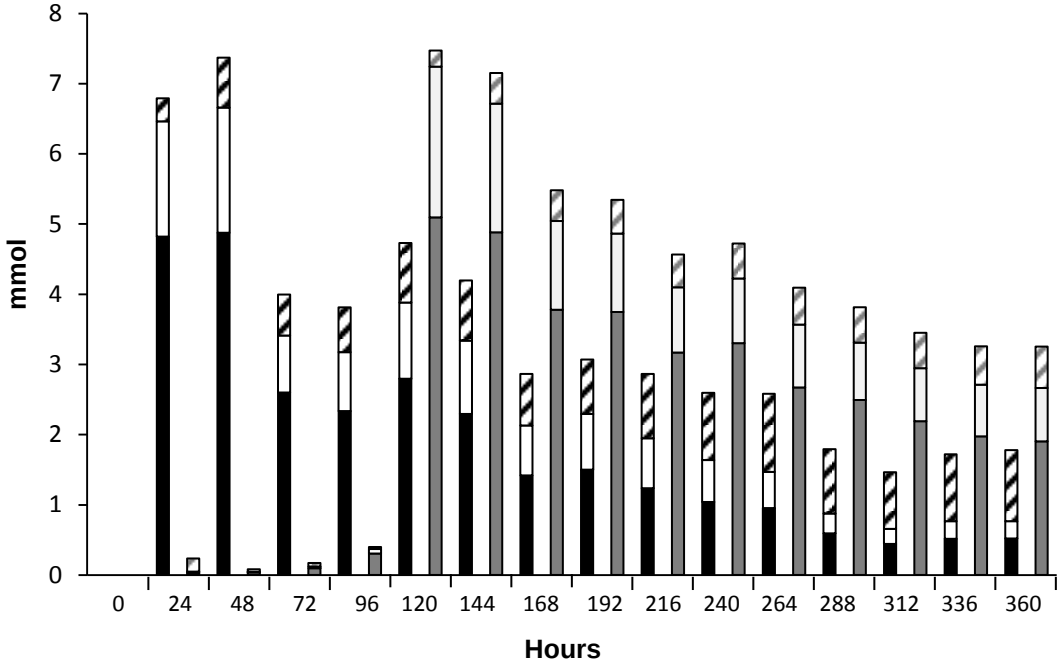

Fig 3. The daily production of volatile components collected in a D_2O trap. Black blocks, on the left show the degradation at 150 °C , grey blocks to the right show the degradation at 90 °C. Solid block = formic acid, clear = acetic acid, patterned = propionic acid.

At 150 °C the majority of acids were given off in the first 48 hours, after this point the rate of acid formation gently reduced over the remaining time frame. This corresponds with the polyunsaturated FAME components being consumed. At first formic acid is the major product, followed by small amounts of both acetic and propionic acid. This profile changes as the test progresses and by 264 hours the majority of volatile acids produced are propionic. This suggests that the primary decomposition of the bisallylic sites produces

formic acid but this mechanism is replaced further into the reaction by the breakdown of secondary oxygenates which yield larger organic acids.

In the 90 °C test, very little acid is observed after 24 hours, this remains low until 120 hours where formic and acetic acids are observed in large quantities. Again, this corresponds with the decomposition of 18:2 and 18:3. The production of volatile acids is remarkably similar to that observed at the higher temperature after this point, although less propionic acid is formed than at 150 °C. Despite the sluggish start at the lower temperature, where presumably the antioxidant is being consumed, overall a similar amount of acids are produced in both tests. This suggests that the original pathways responsible for the formation of acids are not particularly sensitive to temperature and that it is the breakdown of 18:2 and 18:3 which is primarily responsible for the formation of these acids.

The ^{1}H NMR of the D_2O traps show that more than one organic acid is produced through a variety of mechanisms and the pH of the solution will differ depending on the temperature of the accelerated test and the FAME profile. It should also be noted that not all the formic acid will be collected and it reacts with other components in the mixture with the rate of this formation being dependent on the temperature of the accelerated test.

3.2 GC-MS

A further method of following the decomposition of the FAME samples is via GC-MS. Using this technique 16:0, 18:0, 18:1, 18:2 and 18:3 could all be quantified. In this technique the saturated esters were shown not to degrade to any significant degree and still remained in high concentrations after 360 hours (fig. 4). The degradation of 18:1, 18:2 and 18:3 were all quantified and the degradation rates correlate precisely with what was observed in the ^{1}H

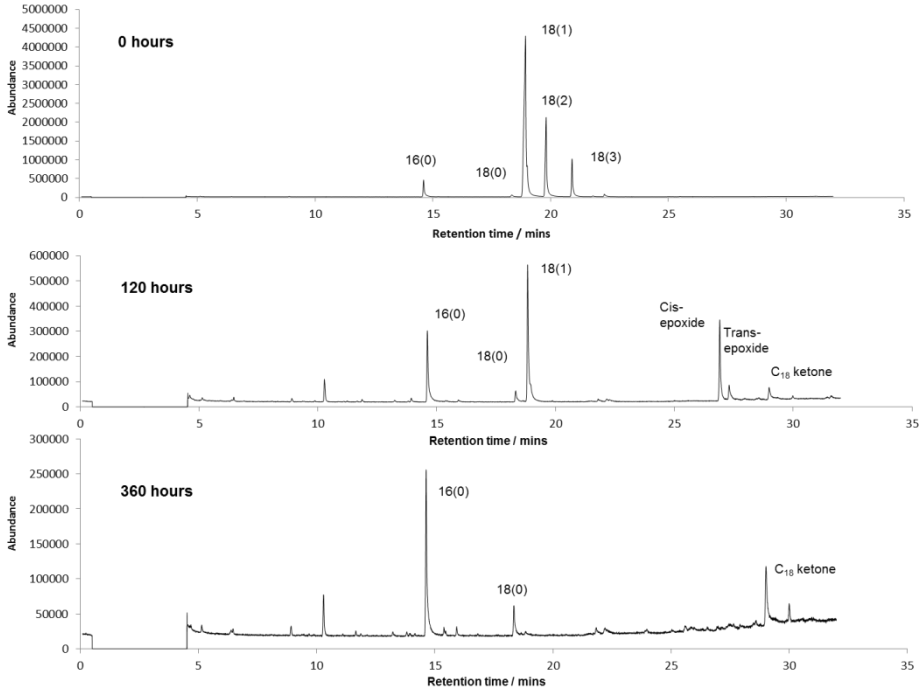

Fig. 4 GC-MS chromatogram for the degradation of RME at 150 °C taken at 0, 120 and 360 hours.

NMR spectra (fig. 5a). Interestingly the degradation rates of 18:2 and 18:3 are highly similar under both reaction conditions after the antioxidant had been consumed.

As the degradation progresses, over 50 organic products can be observed in the GC-MS chromatograph. Most of the peaks were unassignable with any confidence due to their low concentrations, however, from this complexity three major peaks were able to be selected, assigned and quantified (fig. 5b). Under both reaction conditions the onset of degradation of 18:1 correlates with the formation of both a cis- and trans- epoxide. When there is no 18:1 left in the reaction pot, the quantity of epoxide plateaus and, in the 150 °C reaction, subsequently reduces steadily to 0. This epoxide is replaced by an increasing amount of oxygenated components including the C_{18} ketone, methyl 10-oxooctadecanoate. The ketone is only observed after the beginning of the decomposition of the C_{18} epoxides and presumably is the major decomposition product of these components. The identity of the ketone was confirmed by HMQC NMR experiment (see supporting information). It is

therefore likely that the major mechanism of 18:1 decomposition is for the bond to partially isomerise followed by the formation of an epoxide which then forms a ketone.

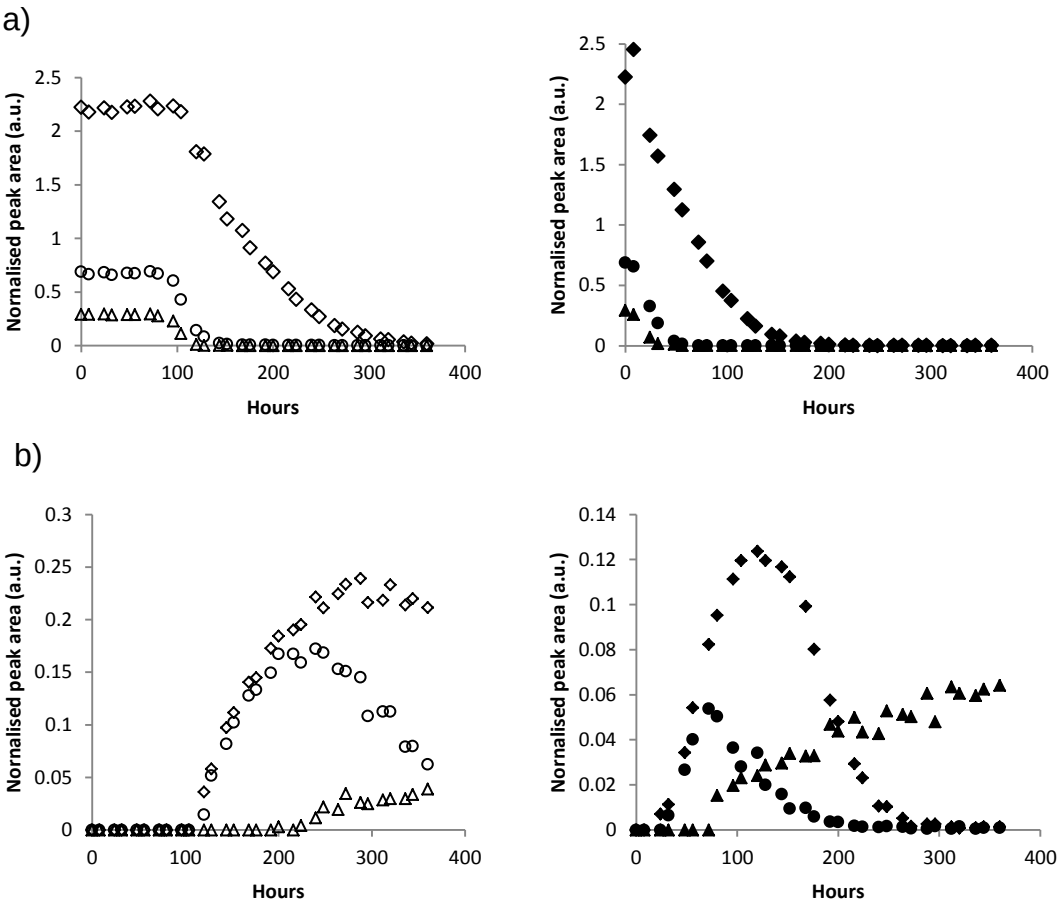

Fig 5. a) GC-MS data showing the degradation of 18(1), ◊, 18(2), ○ and 18(3), Δ. b) GC-MS data showing the formation of a C_{18} cis-epoxide, ◊, a C_{18} trans-epoxide, ○ and Methyl 10-oxooctadecanoate, Δ. Clear blocks show the degradation at 90 °C, solid at 150 °C.

During the accelerated oxidation of biodiesel, the depletion of the antioxidant is dependent on temperature. After the antioxidant has been consumed, the decomposition of the major unsaturated FAME components was highly similar regardless of the temperature. As with previous reports, it was found that the saturated FAMEs are highly stable and while the monounsaturated components do undergo oxidation, they do so at a

slower rate than the polyunsaturated FAME components. The polyunsaturated FAMEs, 18:3 and 18:2, breakdown and form formic acid, alcohols, saturated aldehydes and unsaturated trans aldehydes. These results support the formation of peroxide oligomers as the major pathway to polyunsaturated degradation. The components that are formed further react to produce a range of other volatile acids and oxygenates.

3.3 UV-VIS Spectroscopy

FAME absorbs in the ultraviolet range, though the absorbance spectra vary depending on the FAME profile [17]. Peaks were observed at 245 and 275 nm prior to the onset of oxidation (fig. 6). These peaks increase in amplitude as the samples are heated. A previous report has demonstrated the applicability of these peaks to the level of oxidation [18]. Although reports have tentatively assigned these peaks to conjugated dienes and ketones in the lipid feedstock, no other analytical technique supports that assumption from this work, and the reality is presumably more complex.

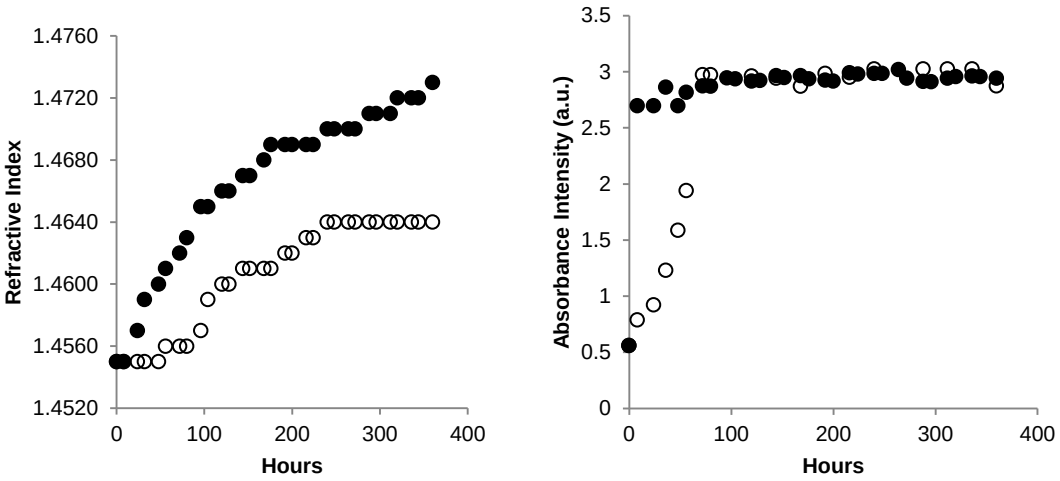

Fig. 6. Refractive index, left, and UV-VIS absorbance intensity plot (275 nm), right, solid blocks show degradation at 150 °C, clear at 90 °C.

As a technique for sensing degradation UV-VIS spectroscopy is limited, as the peaks discussed quickly reach a maximum after only a few hours of degradation time, observable at both 90 and 150 °C. Rather the UV-VIS spectra seems to be useful as an early warning to degradation, if the maximum absorbance has been reached then it can be assumed that there is no antioxidant present in the sample and that the degradation reaction is underway, though by no means advanced, necessitating additional antioxidant.

3.4 Refractive Index

All FAME types have a characteristic refractive index, and therefore there is no single value which determines whether a sample has succumbed to oxidation. In general, the refractive index decreases with increasing saturation as well as decreasing with decreasing chain length [17]. It was therefore a surprise that the refractive index of the oxidised samples increases with oxidation (fig. 6). The increase in the refractive index correlates strongly with the increase in the integral value for the FT-IR fingerprint region (700-1400 cm^{-1}). The RI plot for the oxidation reaction at 90 °C corresponds closely with the ^{1}H NMR of the volatiles in D_2O with a slight increase from 56 hours to 120 hours being observed followed by a rapid increase until 240 hours. The RI then remains constant. The difference in the RI at both temperatures is similar to the difference in the dynamic viscosity (fig. 7), suggesting that, although no real structural information can be obtained from this measurement, the RI is still applicable in tracking the oxidation of biodiesel.

3.5 Dynamic Viscosity

An increase in viscosity is one of the key issues in replacing diesel with biodiesel, during oxidation this issue is exacerbated and the viscosity increases substantially over the reaction time (fig. 7).

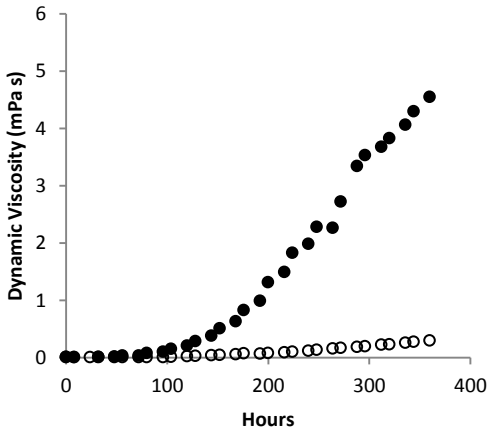

Fig. 7. Dynamic viscosity of the 90 °C oxidation (○) and 150 °C oxidation (●) determined at 15 °C.

The increase in viscosity follows a fairly smooth increase at 150 °C whereas a lag time of 96 hours is observed at 90 °C. At 150 °C the viscosity increases to over 1000 times that of diesel fuel, but this increase is not nearly so great in the 90 °C oxidation reaction. The onset of a rapid increase in the viscosity corresponds with the formation of the larger breakdown products from the 18:1 epoxide formation (fig. 3b). The major decomposition route appears to be via isomerisation and epoxidation rather than a peroxide oligomer mechanism. Though epoxides can be ring-opened by water, an alcohol or other components in the reaction mixture the major product of the epoxide degradation appears to be a saturated ketone. It is only once all the unsaturates have reacted that the viscosity increases to extreme levels. This suggests that although the breakdown of polyunsaturates produces more saturated components than present in the original biodiesel, the viscosity increase due to these compounds is negligible and it is only the oligomers, resulting from the

reaction of secondary oxidation products that cause the viscosity increase. The observed viscosity increase is much lower in the 90 °C reaction which suggests there are far fewer high molecular weight components formed. This is one of the key differences in using higher temperatures in accelerated testing. This large increase in the viscosity is of particular concern when considering biodiesel present in the engine sump oil where these temperatures, and increased amounts of biodiesel, are observed in vehicles fitted with a DPF system.

3.6 Gel Permeation Chromatography

The final samples for both oxidations carried out at 90 °C and at 150 °C were analysed by GPC and the elution times compared to that of RME (fig. 8).

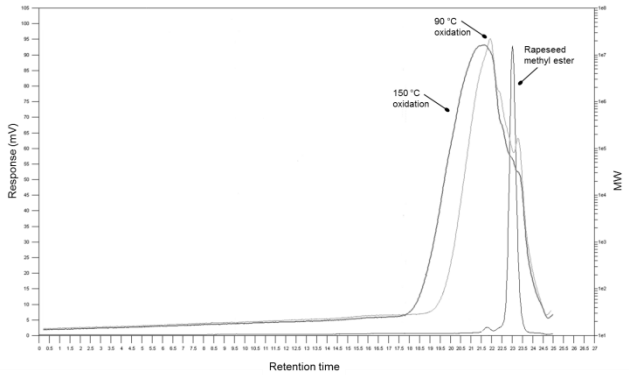

Fig. 8. GPC chromatograph of rapeseed methyl ester, oxidised biodiesel from the 90 °C reaction (grey) and from the oxidation carried out at 150 °C (black) after 360 hours.

The RME started to elute after 22.5 minutes and contained one well defined peak. This is consistent with the low molecular weight of the components and relative purity of the sample. On oxidation at 90 °C the peak broadens substantially and the oxidised biofuel starts to elute after 19 minutes. This suggests that a substantial number of oxidised

compounds are formed, most of which have a higher molecular weight than that of the original RME. In the 150 °C reaction this effect is more pronounced and the sample starts to elute quicker still at 17.5 minutes, suggesting that there are more higher molecular weight oxygenates than observed at 90 °C. This analysis suggests that the increase in viscosity is due to the formation of higher molecular weight oligomers.

3.7 FT-IR Spectroscopy

FT-IR spectroscopy has been previously used in analysing the degradation of waste cooking oil methyl ester [19].

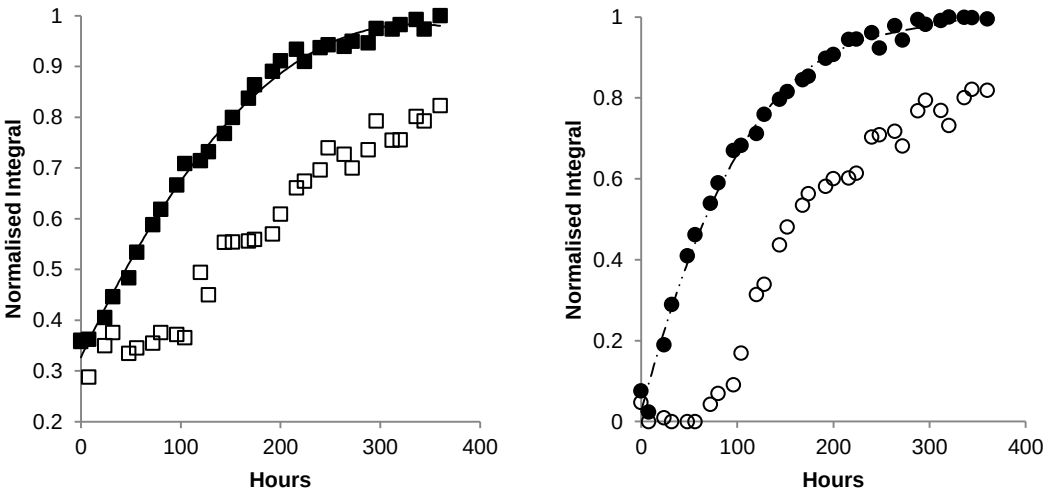

Fig. 9. Normalised Integral FT-IR values for the carbonyl stretch integrated from 1650 cm^{-1} – 1800 cm^{-1} at 150 °C (■) and 90 °C (□) and for the fingerprint area 700 – 1400 cm^{-1} at 150 °C (●) and 90 °C (○). All trend lines are polynomial fits with r^2 values greater than 0.99.

The carbonyl stretch at 1740 cm^{-1} can be seen to expand as the decomposition progresses as more carbonyl containing compounds such as ketones, aldehydes and acids are produced in the reaction mixture. The O-CH_3 stretch observed at 1240 cm^{-1}, as well as the fingerprint

region in general, enlarges as the reaction time continues. This is presumably due to the proportional increase in the amount of ester and C-H single bonds in the reaction mixture as the unsaturated components degrade into volatile oxygenates. By integrating these peaks (700-1400 cm^{-1}) over a wide range, this effect can be quantified (fig. 9). The data presented correlates strongly with the reduction in double bonds observed in the NMR spectra, as well as the formation of volatile compounds. Previous investigations have qualified the degradation by the cis bond stretch observable at 710 cm^{-1} [19]. Although this peak was observed at low temperatures soon after the onset of oxidation, it was not able to be integrated to quantify the oxidation.

Though more information can be garnered from the GC-MS and ^{1}H NMR spectra, they rely on extensive sample preparation and therefore are not ideal for online kinetics or sensor technology. To this end it is suggested that FT-IR, over the RI, UV or rheometry is the most suitable technique for this type of analysis.

4. Conclusions

The oxidation of biodiesel can be most accurately assessed in depth using GC-MS or ^{1}H NMR spectroscopy on a laboratory timescale, though FT-IR was found to be the most relevant for sensor technology. The onset of the degradation is highly dependent on temperature though the rate of decomposition and the identity of the primary oxidation products formed were less so. The final viscosity of the samples differed greatly depending on the temperature, though in both tests a similar amount of biodiesel had degraded. This is the major issue with using accelerated tests to simulate real world conditions.

5. Acknowledgements

We would like to acknowledge the EPSRC for funding various aspects of this work, through the Doctoral Training Centre at the Centre for Sustainable Chemical Technologies as well as the FORD Motor Company and BP for additional funding, advice and supplying the RME.

6. References

[1] Bannister, C. D.; Chuck, C. J.; Bounds, M.; Hawley, J. G. Oxidative stability of biodiesel fuel Proc Inst Mech Eng Part D-J Automob Eng 2011; 225, 99.

[2] Chisti, Y. Biodiesel from microalgae. Biotechnol Adv 2007; 25, 294.

[3] Dunn, R. O. Oxidative stability of biodiesel by dynamic mode pressurized-differential scanning calorimetry (P-DSC). Trans ASABE 2006; 49, 1633.

[4] Dunn, R. O. Effect of oxidation under accelerated conditions on fuel properties of methyl soyate (biodiesel). J Am Oil Chem Soc 2002; 79, 915.

[5] Fang, H. L.; Whitacre, S. D.; Yamaguchi, E. S.; Boons, M. Biodiesel impact on wear and protection of engine oils. SAE technical paper series 2007; 2007-01-4141.

[6] Thornton M.J., Alleman T.L.; Luecke J. and McCormick R.L. Impacts of Biodiesel Fuel Blends Oil Dilution on Light-Duty Diesel Engine Operation. SAE Int J Fuels Lubr 2009; 2, 1, 781

[7] Andreae M.; Fang H. and Bhandary K. Biodiesel and Fuel Dilution of Engine Oil. SAE technical paper series 2007; 2007-01-4036

[8] Knothe, G. Some aspects of biodiesel oxidative stability. Fuel Process Technol 2007; 88, 669.

[9] Monyem, A.; Canakci, M.; Van Gerpen, J. H. Investigation of biodiesel thermal stability under simulated in-use conditions. Appl Eng Agric 2000; 16, 373.

[10] Morita, M.; Tokita, M. The real radical generator other than the main product hydroperoxide in lipid autoxidation. Lipids 2006; 41, 91.

[11] Schneider, C.; Porter, N. A.; Brash, A. R. Routes to 4-hydroxynonenal: Fundamental issues in the mechanisms of lipid peroxidation. J Biol Chem 2008; 283, 15539.

[12] Bannister, C. D.; Chuck, C. J.; Hawley, J. G.; Price, P.; Chrysafi, S. S. Factors affecting the decomposition of biodiesel under simulated engine sump oil conditions. Proc Inst Mech Eng Part D-J Automob Eng 2010; 224, 927.

[13] Knothe, G. Analysis of oxidized biodiesel by H-1-NMR and effect of contact area with air. Eur. J Lipid Sci Technol 2006; 108, 493.

[14] Fang, H. L.; McCormick, R. L. Spectroscopic study of biodiesel degradation pathyways. SAE technical paper series 2006; 2006-01-3300.

[15] Jain, S.; Sharma, M. P. Review of different test methods for the evaluation of stability of biodiesel Renew. Sust Energ Rev 2010; 14, 1937.

[16] Ogawa, T.; Kajiya, S.; Kosaka, S.; Tajima, I.; Yamamoto, M.; Okada, M. Analysis of Oxidative Deterioration of Biodiesel Fuel. SAE technical paper series 2008; 2008-01-2502.

[17] Chuck, C. J.; Bannister, C. D.; Hawley, J. G.; Davidson, M. G. Spectroscopic sensor techniques applicable to real-time biodiesel determination. Fuel 2010; 89, 457.

[18] Dantas, M. B.; Albuquerque, A. R.; Barros, A. K.; Rodrigues Filho, M. G.; Antoniosi Filho, N. R.; Sinfronio, S. M.; Rosenhaim, R.; Soledade, L. E. B.; Santos, I. M. G.; Souza, A. G. Evaluation of the oxidative stability of corn biodiesel. Fuel 2011; 90, 773.

[19] Furlan, P. Y.; Wetzel, P.; Johnson, S.; Wedin, J.; Och, A. Investigating the Oxidation of Biodiesel From Used Vegetable Oil by FTIR Spectroscopy: Used Vegetable Oil Biodiesel Oxidation Study by FTIR. Spectr Lett 2010; 43, 580.

Supplementary information

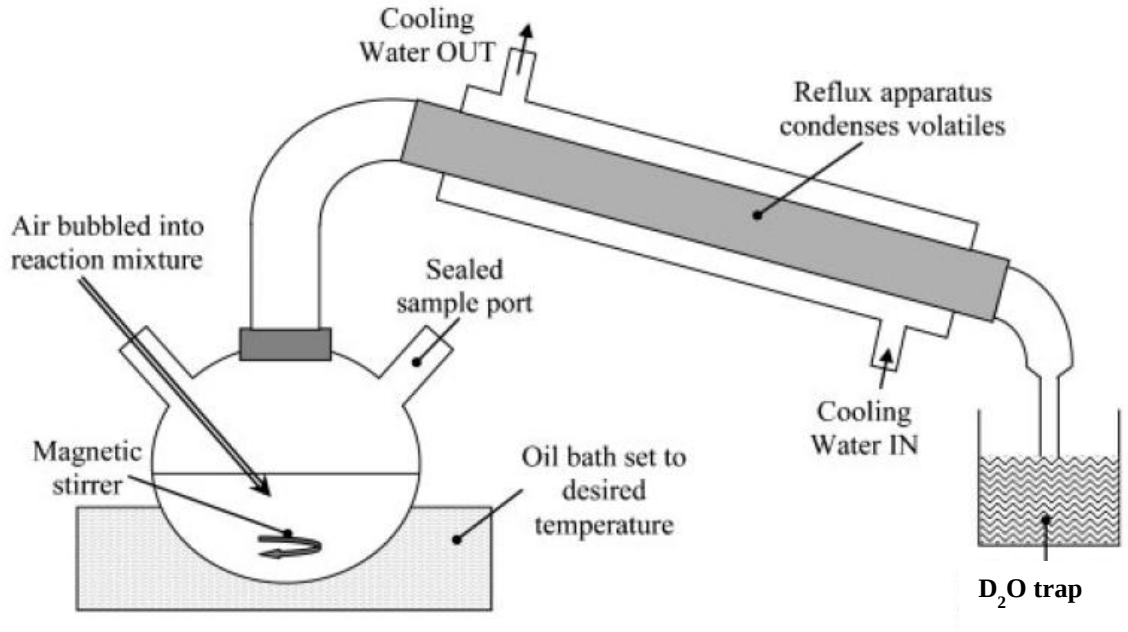

Fig. S1 Diagram of apparatus set up used in the oxidation of RME

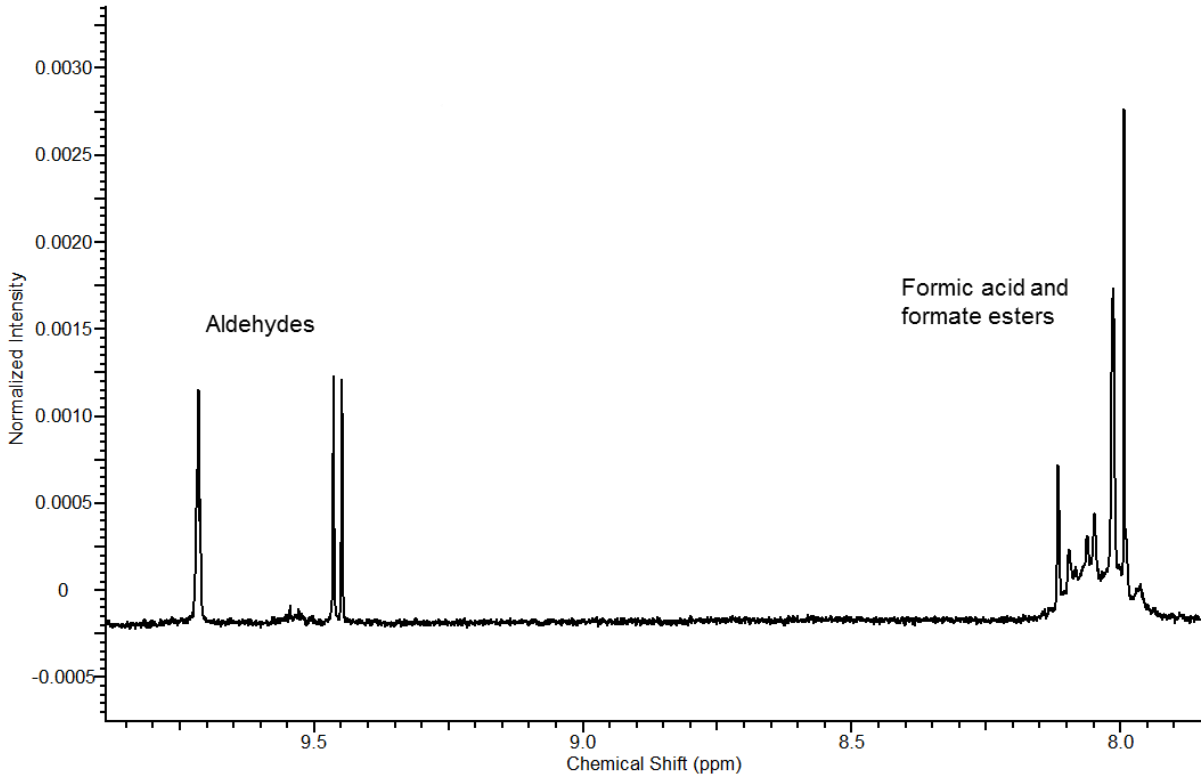

Fig. S2 ^{1}H NMR spectra of the oxidation of RME at 150 °C of the sample taken at 96 hours

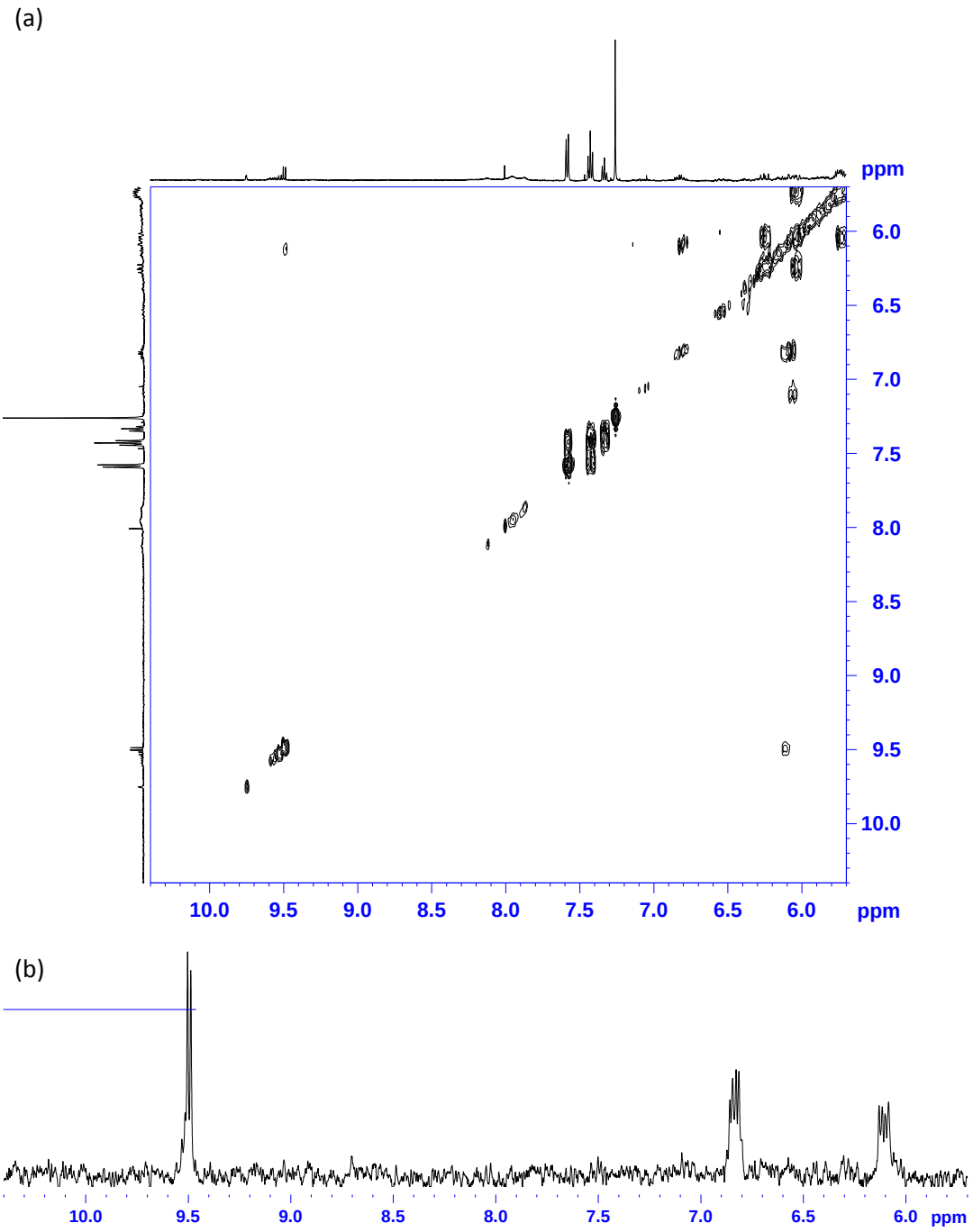

Fig. S3 (a) ^{1}H-^{1}H COSY and (b) 1D ^{1}H TOCSY (selectively excited at δ 9.50 ppm) NMR spectra, taken at 24 hours into the oxidation of RME at 150 °C , showing the identity of a trans unsaturated aldehyde. Only the region between δ 10.4 and δ 5.7 ppm is shown.

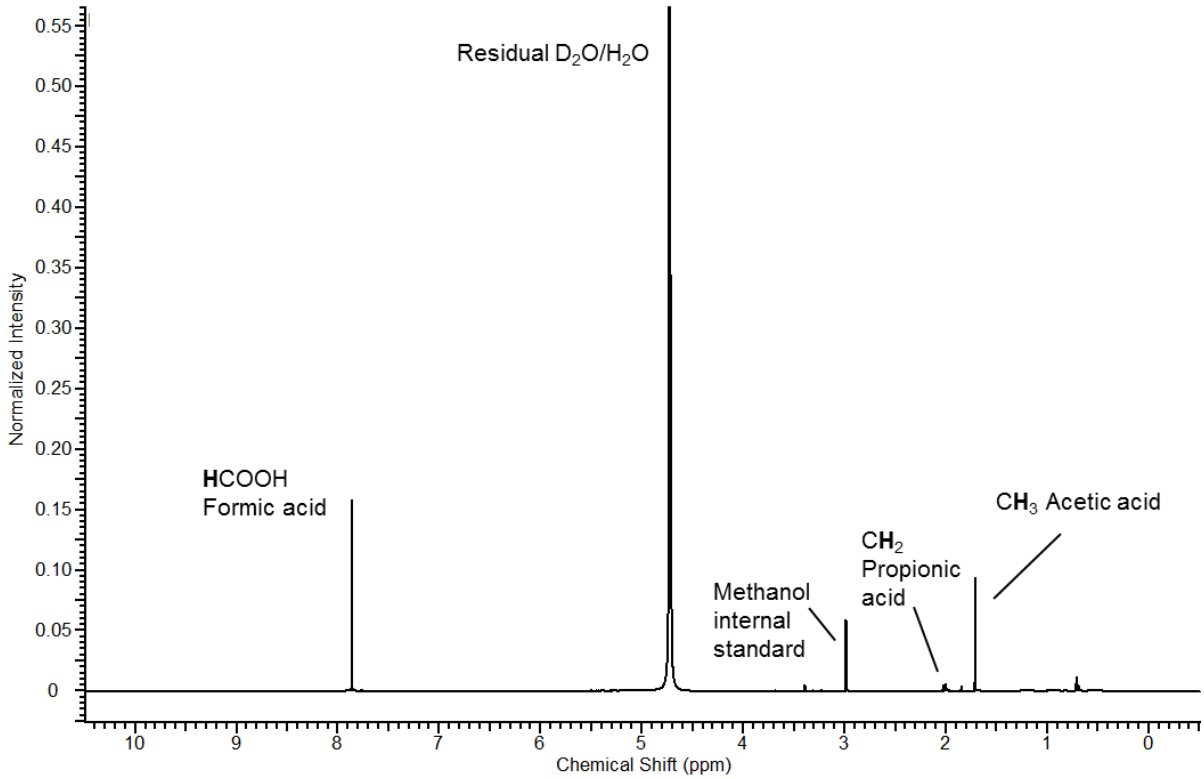

Fig. S4 ^{1}H NMR spectra of the D_2O trap, collected after 24 hours for the oxidation of RME at 150 °C

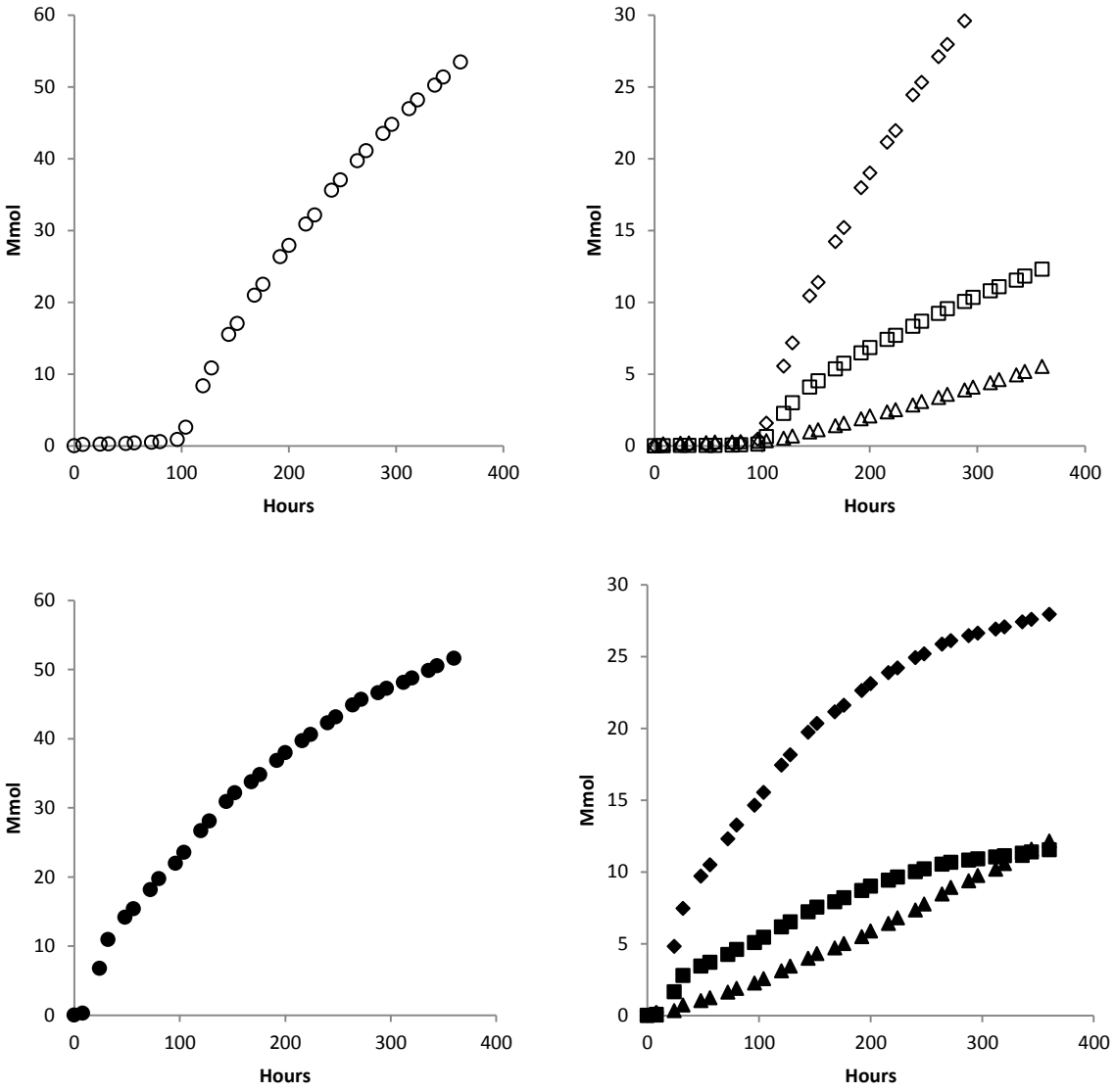

Fig. S5 Accumulated data derived from the ^{1}H NMR spectra of the D_2O trap, showing total molar volume of acids, (○), formic acid, (◊), acetic acid (□) and propionic acid (Δ). Solid blocks show the degradation at 150 °C, clear at 90 °C.

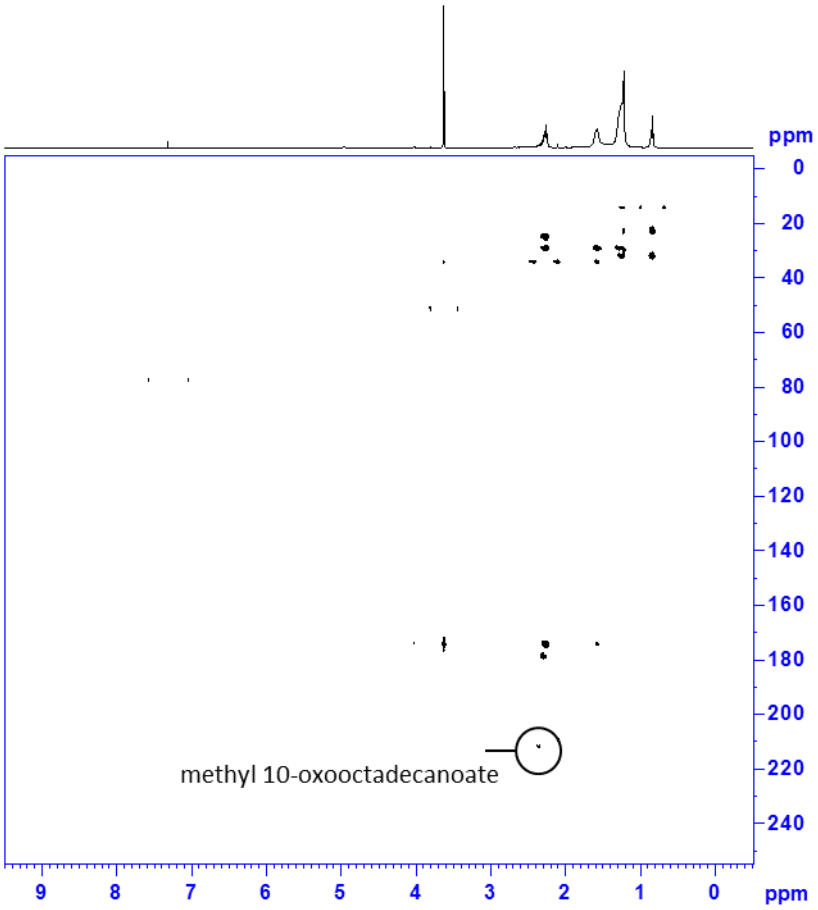

Fig. S6 ^{1}H-^{13}C HMQC NMR spectra, taken at 360 hours into the oxidation of RME at 150 °C , confirming the identity of methyl 10-oxooctadecanoate

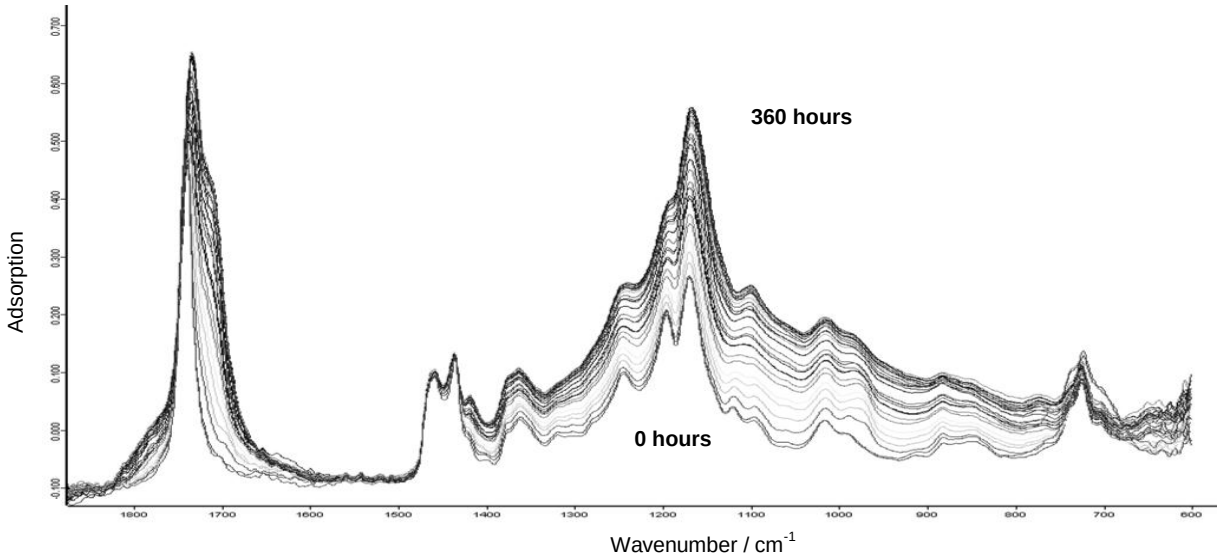

Fig. S7 Time resolved FT-IR spectra from 0 – 360 hours, showing the broadening of the carbonyl peak and the general increase in the adsorption across the fingerprint region, for the oxidation at 150 °C

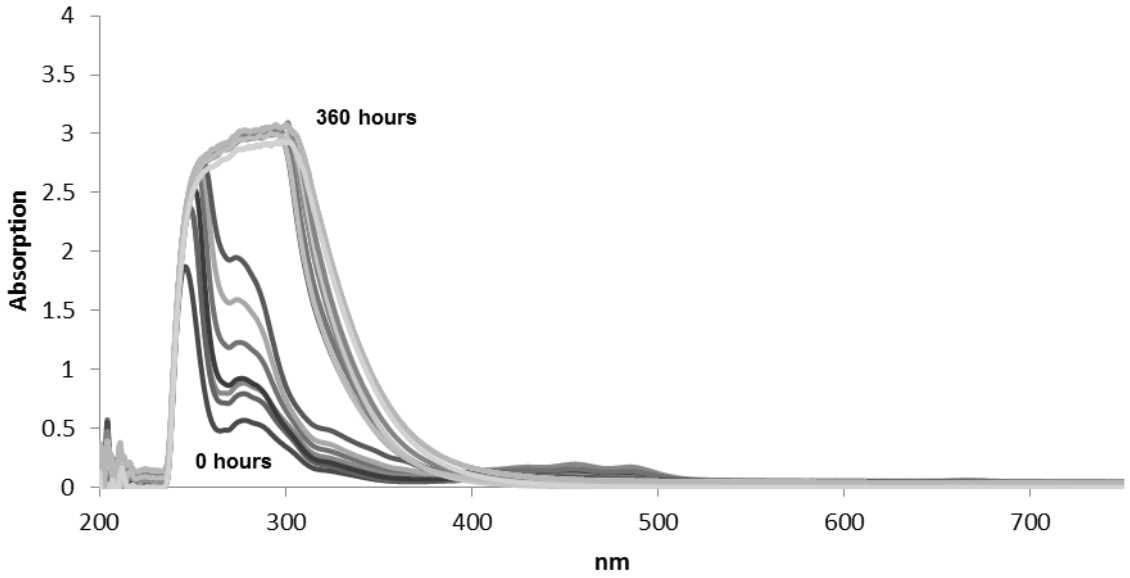

Fig. S8 Overlaid UV-Vis spectra from 0-360 hours for the degradation of RME at 90 °C

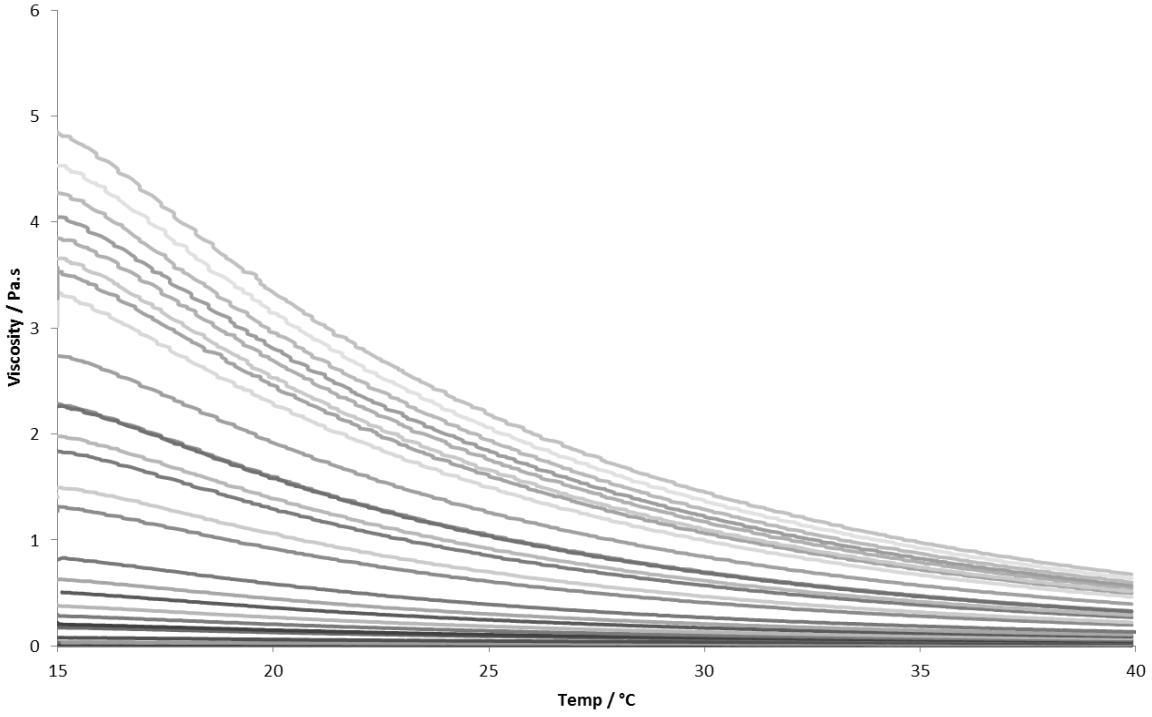

Fig. S9 Dynamic viscosities of the samples taken from 0 – 360 hours in the oxidation of RME at 150 °C.